ISSN 1990-4789, Journal of Applied and Industrial Mathematics, 2021, Vol. 15, No. 2, pp. 223–233. © Pleiades Publishing, Ltd., 2021.
Russian Text © The Author(s), 2021, published in Sibirskii Zhurnal Industrial'noi Matematiki, 2021, Vol. 24, No. 2, pp. 62–76.

Modeling Regular Textures in Images Using the Radon Transform

I. G. Kazantsev[1*], R. Z. Turebekov[2], and M. A. Sultanov[2***]**

[1] *Institute of Computational Mathematics and Mathematical Geophysics, pr. Akad. Lavrentyeva 6, Novosibirsk, 630090 Russia*

[2] *Khoja Akhmet Yassawi International Kazakh-Turkish University, pr. Bekzat Sattarkhanova 29, Turkestan,161200 Kazakhstan*

Received December 2, 2020; in final form, February 3, 2021; accepted April 15, 2021

Abstract—The Radon transform is a major integral transform in computed tomography and a widely applied technique in computer vision and image analysis which is used to detect linear structures and regular textures. Its application is based on the property of the integrals of the direct problem to accumulate the image brightness along the contours under study. The back-projection operation, one of the main components of tomographic algorithms, results in ridge functions having the directions in which they participated in the direct operator. In the present paper, we examine the ridge functions and their orientation as the features for describing the anisotropy of regular textures. These features are involved in the regular texture model as a sum of ridge functions. Many textures are visually perceived as a superposition of linear structures and are therefore examined using the Radon transform. The paper presents a computational scheme for the singular value decomposition of a regular texture into a sum of informative ridge functions. The results are given of numerical experiments with the textures of industrial fabrics. The algorithm can be used in processing the visual data in computer vision systems, textile industry, robotics, and crystallography.

DOI: 10.1134/S1990478921020046

Keywords: *image processing, Radon transform, regular texture, textile*

INTRODUCTION

The Radon transform is a major integral transform in computed tomography [1] and is also a widely applied method in machine vision and image analysis which is used to detect linear structures and regular textures. Application of the Radon transform to find boundaries in the form of parameterized curves (lines, ellipses, etc.) on the digital images is called the Hough transform [2], whereas the linear structures are called "lineaments" [3, 4]. Information about the presence of curved objects is contained in the data calculated from this image, which includes the integrals along some curves that coincide with the desired structures because these integrals accumulate the same (approximately) values along their contours. In particular, in the problem of finding linear structures, the presence of a straight line manifests itself in local extremes on a sinogram; i.e., a visualized image of the Radon transform. A mathematical generalization of linear structures is ridge functions that were first defined in [5] and surveyed in [6–8]. Here we use the ridge functions and their orientation as the features to describe anisotropy of some important objects in the images such as regular textures. These features are included in the model of many regular textures as a sum of ridge functions.

Textures are subdivided into the two classes: stochastic and regular ones [9, 10]. A *stochastic texture* is a random field of brightness in which the construction elements cannot be described analytically, and thus the statistical methods of signal processing are more suitable [11]. Some examples of a stochastic

[*] E-mail: kazantsev.ivan6@gmail.com
[**] E-mail: rauan.turebekov@ayu.edu.kz
[***] E-mail: murat.sultanov@ayu.edu.kz

texture are "white" noise on the TV screen, ripples on the surface of the reservoir during rain, pictures of tree crowns from a height, etc.

The object of analysis in the present study involves *regular textures*. Along with this term, "ornament," "pattern," and "structure" can also be used; among common examples are brickwork, parquet, lattices, weaves, textiles, banknotes, etc. In computer vision applications [12–14] such as automatic control of materials, the detection of defects in textures has become a separate area of image analysis. The reader can get the idea of wide range of the relevant topics from many surveys and monographs (for instance, see [15–20]).

Defects in the texture are the areas of local random violation of the fabric pattern periodicity. Traditionally, the defects were detected by visual inspection with the participation of a human inspector; this takes rather long time and does not provide accuracy. For an objective and consistent assessment, there are used the automated control systems based on computer vision. The automated fabric inspection offers many advantages including the increased safety, the reduced costs, the elimination of human errors and makes it possible to carry out separately the actual production and the fabric control. Over the past decades, various methods has been developed of automatic fabric control such as the monitoring the spatial frequency spectrum of the fabric [21], some variational methods [22], wavelet analysis [23], the low-rank representations of textures [24], methods of the theory of lattices and coverings [25], the deep learning of neural networks [26], regression analysis [27], etc.

The identification of textures in the images in the present work is based on a quantitative criterion for the informative value of the integral data of the Radon transform. In the experiments with some industrial samples of textile textures, it is shown that the decomposition of a regular texture into the sum of small number (4–8) of the most informative ridge functions gives a good approximation of the texture. This technique can monitor the texture images in computer vision systems and detect some structureless inclusions on them.

The article is organized as follows:

In Section 1, some definitions are introduced and the main provisions and statements are introduced that are necessary to justify the analysis of regular textures in the Radon space. In Section 2, the method of singular value decomposition of the Radon transform is described. In Section 3, a criterion is found for the informative value of projections for determining the prevailing directions in the texture. In Section 4, a computational scheme for decomposing textures into the sum of ridge functions is discussed. In Section 5, the results of testing the method on texture images from some open image databases are presented.

1. RADON TRANSFORM

Let us introduce the definition of Radon transform [1] and give some highlights and main statements that are necessary to justify the analysis of regular textures using the Radon transform.

Definition 1. The (two-dimensional) *Radon transform* R is defined as the operator that maps a function f on $\mathbb{R}^2$ to the set of the straight-line integrals of f in $\mathbb{R}^2$:

$$Rf(\theta, s) \equiv p(\theta, s) = \int\limits_{\langle u,\theta\rangle = s} f(u)\, du = \int\limits_{-\infty}^{\infty} f(s\theta + t\theta^{\perp})\, dt, \tag{1}$$

where $\theta = \theta(\alpha) = (\cos\alpha\ \ \sin\alpha)^{\top} \in \mathbb{S}^1$ is some unit vector, α is the angle between θ and the positive axis y, while $\theta^{\perp} = (-\sin\alpha\ \ \cos\alpha)^{\top}$ is perpendicular to θ, and $s \in \mathbb{R}^1$.

The *inverse Radon transform* [1] acting on the data $p = Rf$ has the form

$$f = \frac{1}{4\pi}\, R^{\#}\mathbb{H}\frac{\partial}{\partial s}\, p, \tag{2}$$

where $\mathbb{H}$ denotes the Hilbert transform in the second variable

$$\mathbb{H}p(\theta, s) = \frac{1}{\pi} \int\limits_{-\infty}^{\infty} \frac{p(\theta, t)}{s - t}\, dt. \tag{3}$$

Here $R^{\#}$ is the *back-projection operator*

$$R^{\#}p(u) = \int_0^{2\pi} p(\theta, \langle u, \theta\rangle)\, d\alpha. \tag{4}$$

Given some fixed θ, the function $p(\theta, \langle u, \theta\rangle)$ is constant on straight lines perpendicular to θ.

Recall the definition of ridge functions [5–8]:

Definition 2. Let $D \subset \mathbb{R}^2$. A *ridge function* on D is understood as a function of the form $\varphi(\langle a, x\rangle)$, where $x = (x_1, x_2) \in D$, $a = (a_1, a_2) \in \mathbb{R}^2 \setminus \{0\}$, and φ is a real-valued function.

The function $p(\theta, \langle u, \theta\rangle)$ is a ridge function, and the equations (2)–(4) describe the representation of the function f as a sum of ridge functions. These formulas are the basis of the filtered back-projection (FBP) method in which the operator

$$(1/4\pi)\mathbb{H}\left(\frac{\partial}{\partial s}\right)$$

is approximated by the convolution operator with kernel k; and as a result, the reconstruction algorithm has the form

$$f = R^{\#}(k * p), \qquad (k * p)(\theta, s) = \int_{-\infty}^{\infty} k(s - t)p(\theta, t)\, dt.$$

The above formulas essentially use the complete data with respect to θ and s. In practice, this data is discrete, and the transition from sample values to complete data remains to be a topical problem. We assume that the functions f are interpreted as images with a disc-shaped support.

Let f be a square-integrable function whose support D is a disc of the unit radius on the plane (x, y); i.e., $f \in L_2(D)$. It is convenient to use the parametrization of the projection direction $p(\theta, s)$ not by the vector $\theta = \theta(\alpha) = (\cos\alpha \ \ \sin\alpha)^\top$ but using the angle α, which this vector forms with the positive direction of the y axis. In this case, the short expression "projection $p(\alpha, s)$ in the direction α," widely used in the literature, is understood as $p(\theta, s)$. The transform maps f to its integrals along some bundle of parallel lines parameterized by the angle $\alpha \in [0, \pi)$ and the distance $s \in [-1, 1]$ from the origin. Equation (1) can be written with the specified limits of integration:

$$R_\alpha f(s) = \int_{-\sqrt{1-s^2}}^{\sqrt{1-s^2}} f(s\cos\alpha - t\sin\alpha, s\sin\alpha + t\cos\alpha)\, dt.$$

The operator $f \mapsto R_\alpha f$ is continuous when the spaces $L_2(D)$ and $L_2([-1, 1], (1 - s^2)^{-1/2})$ are considered. An individual projection will also be denoted as $p(\alpha, s) = p_\alpha(s)$. Formula (2) assumes all $p(\alpha, s)$, given on $[0, \pi) \times [-1, 1]$, to be known. In practical situations of computed tomography, data is represented by a finite set of projections and finitely many samples per a projection. We will call a projection *complete* if it is known on the entire segment $[-1, 1]$. If the set of projection directions is represented by an n-vector $\omega = (\omega_1, \ldots, \omega_n) \in [0, \pi)^n$ then the corresponding set of complete projections is denoted as

$$R_\omega f = (R_{\omega_1} f, \ldots, R_{\omega_n} f).$$

In the tomographic scanners registering some sufficient number of projections equally distributed with respect to the angles, the reconstruction of the function f from the data $R_\omega f$ is carried out as a sum of filtered back-projections (FBP):

$$f(x, y) \approx \sum_{i=1}^{n} r_i(x\cos\omega_i + y\sin\omega_i) = \sum_{i=1}^{n} r_i((x, y) \cdot (\cos\omega_i \ \ \sin\omega_i)^\top). \tag{5}$$

The functions r_i are defined as

$$r_i(s) = \int_{-\infty}^{\infty} p(\omega_i, t)k(s-t)\,dt.$$

The convolution kernel k is a regularized version of the inverse Fourier transform of the spatial frequency modulus $|\xi|$. We should note that the same k is used for each r_i. The FBP method is also closely related to the inversion methods based on the Fourier transform and the Central Section Theorem. This theorem states that the one-dimensional Fourier-image of $\hat{p}(\theta, \xi)$ of the projection data $p(\theta, s)$ is equal to the central section of the two-dimensional Fourier image $\hat{f}$ in the direction $\theta^{\perp}$. Formula (5) expresses the approximation of f as the sum of the ridge functions r_i with the directions ω_i uniformly distributed in the interval $[0, \pi)$.

2. SINGULAR VALUE DECOMPOSITION OF THE RADON TRANSFORM

However, in the case of an arbitrary set of directions ω, as well as in the case of rather few of them, an approach based on the following existence theorem [5] is preferable among the analytical methods:

If H is a function in $L_2(D)$ with the minimal norm satisfying the conditions

$$R_{\omega_i} f = R_{\omega_i} H, \qquad i = 1, \ldots, n; \tag{6}$$

then there exist functions $h_1, \ldots, h_n \in L_2\big([-1,1], (1-s^2)^{-1/2}\big)$ such that

$$H(x,y) \equiv H_\omega(x,y) = \sum_{i=1}^{n} h_i(x\cos\omega_i + y\sin\omega_i). \tag{7}$$

The functions $h_i(x\cos\omega_i + y\sin\omega_i)$ are ridge functions. The Shepp–Logan Theorem is a statement on the existence of ridge functions in the selected directions. We outline a constructive algorithm for calculating the sum $H_\omega(x,y)$ of the ridge functions from an arbitrary set of complete projections $R_\omega f$. Let $H \in L_2(D)$ be searched as the sum (7) of n ridge functions.

Put $p_i(s) \equiv p(\omega_i, s)$. Equations $R_{\omega_i} H(s) = p_i(s)$, $i = 1, \ldots, n$, form a consistent system equivalent to (6). At the same time, it can be interpreted as a model of generating the projections of p_i for H. Then the problem of reconstructing the function H can be formulated in terms of functions h_i and p_i of a single variable. The proposed approach is based on the following statements:

Proposition 1. *Let $H_\beta(x,y) = h_\beta(x\cos\beta + y\sin\beta)$, where $h_\beta(s) \in L_2([-1,1], (1-s^2)^{-1/2})$. The the projection $R_\alpha H_\beta \equiv R_\alpha[H_\beta]$ of H_β has the form*

$$R_\beta[H_\beta](s) = 2(1-s^2)^{1/2} h_\beta(s), \qquad R_\alpha[H_\beta](s) = \frac{1}{\sin(\alpha-\beta)} \int_{s_1}^{s_2} h_\beta(t)\,dt,$$

where

$$s_1 = s\cos(\alpha-\beta) - (1-s^2)^{1/2}\sin(\alpha-\beta), \qquad s_2 = s\cos(\alpha-\beta) + (1-s^2)^{1/2}\sin(\alpha-\beta).$$

Proof. We have

$$\|H_\beta\|^2_{L_2(D)} = 1/2 \int_{-1}^{1} (1-s^2)^{-1/2} h_\beta^2(s)\,ds < \infty.$$

Then $H_\beta \in L_2(D)$ and the transform R_α is applicable:

$$R_\alpha[H_\beta](s) = \int\limits_{-(1-s^2)^{1/2}}^{(1-s^2)^{1/2}} H_\beta(s\cos\alpha - z\sin\alpha, s\sin\alpha + z\cos\alpha)\,dz$$

$$= \int\limits_{-(1-s^2)^{1/2}}^{(1-s^2)^{1/2}} h_\beta(s\cos(\alpha-\beta) - z\sin(\alpha-\beta))\,dz.$$

The change of variables $t = s\cos(\alpha-\beta) - z\sin(\alpha-\beta)$ proves Proposition 1. □

Proposition 2. *If $H(x,y)$ is the sum of ridge functions then the constraints in the form of the projection data $R_{\omega_i}H = p_i$, $i = 1,\dots,n$ are equivalent to the system of Fredholm integral equations of the third kind*

$$a(s)h_i(s) + \sum_{j=1,\ j\neq i}^{n} \frac{1}{\sin(\omega_i-\omega_j)} \int\limits_{s_1}^{s_2} h_j(t)\,dt = p_i(s), \tag{8}$$

where

$$a(s) = 2(1-s^2)^{1/2}, \quad s\in[-1,1],$$

$$s_1 = s\cos(\omega_i-\omega_j) - (1-s^2)^{1/2}\sin(\omega_i-\omega_j), \qquad s_2 = s\cos(\omega_i-\omega_j) + (1-s^2)^{1/2}\sin(\omega_i-\omega_j).$$

Proof. Put $H_{\omega_j}(x,y) = h_j(x\cos\omega_j + y\sin\omega_j)$. Owing to the linearity of the Radon transform, the constraints take the form

$$R_{\omega_i}\left[\sum_{j=1}^{n} H_{\omega_j}\right](s) = R_{\omega_i}[H_{\omega_i}](s) + \sum_{j=1,\ j\neq i}^{n} R_{\omega_i}[H_{\omega_j}](s).$$

Applying Proposition 1, we obtain (8). The proof is complete. □

Proposition 3. *The Chebyshev polynomials of the second kind*

$$U_{k-1}(t) = \frac{\sin(k\arccos t)}{\sin(\arccos t)}, \qquad k = 1,2,\dots,$$

satisfy the relation

$$\int\limits_{s_1}^{s_2} U_{k-1}(t)\,dt = a(s)\frac{\sin(k\alpha)}{k}U_{k-1}(s),$$

where $s_1 = s\cos\alpha - (1-s^2)^{1/2}\sin\alpha$ and $s_2 = s\cos\alpha + (1-s^2)^{1/2}\sin\alpha$.

Proof. We use the identity $T_k'(t) = kU_{k-1}(t)$, where $T_k = \cos(k\arccos t)$ is the Chebyshev polynomials of the first kind. Substituting $\cos\beta = s$ and $\sin\beta = (1-s^2)^{1/2}$, we obtain

$$\int\limits_{\cos(\beta+\alpha)}^{\cos(\beta-\alpha)} \frac{T_k'(t)}{k}\,dt = \frac{1}{k}[T_k(\cos(\beta-\alpha)) - T_k(\cos(\beta+\alpha))]$$

$$= \frac{2}{k}\sin(k\arccos s)\sin(k\alpha) = \frac{a(s)}{k}U_{k-1}(s)\sin(k\alpha).$$

Proposition 3 is proved. □

Theorem 1. *Let $\omega = (\omega_1, \dots, \omega_n)$ be some n-vector of different angles. Let $f \in L_2(D)$ and let H be a function in $L_2(D)$ with the minimal norm, satisfying the conditions $R_{\omega_i} f = R_{\omega_i} H$ for $i = 1, \dots, n$. Then the functions $h_1, \dots, h_n$ that form the decomposition into the sum of ridge functions*

$$H(x, y) = \sum_{i=1}^{n} h_i(x \cos \omega_i + y \sin \omega_i),$$

can be written in the form

$$h_i(s) = \frac{1}{\pi} \sum_{k=1}^{\infty} \sum_{j=1}^{n} \eta_{ij}^{(k)} U_{k-1}(s) \int_{-1}^{1} p_j(t) U_{k-1}(t)\, dt, \tag{9}$$

where $\eta_{ij}^{(k)}$ are elements of the matrix that is the generalized inverse to $\Lambda_k = \left[\lambda_{ij}^{(k)}\right]$, $i, j = 1, \dots, n$, where

$$\lambda_{ij}^{(k)} = \frac{\sin\bigl(k(\omega_i - \omega_j)\bigr)}{k \sin(\omega_i - \omega_j)}.$$

Proof. We have

$$h_i, p_i \in L_2([-1, 1], (1 - s^2)^{-1/2}) \subset L_2([-1, 1]) \subset L_2([-1, 1], (1 - s^2)^{1/2}).$$

Then putting $v_i(s) = p_i(s)/a(s)$, we have $v_i, h_i \in L_2([-1, 1], (1 - s^2)^{1/2})$ and can use the Chebyshev polynomial expansions of h_i and v_i

$$h_i(s) = \sum_{k=1}^{\infty} b_i^{(k)} U_{k-1}(s), \qquad v_i(s) = \sum_{k=1}^{\infty} c_i^{(k)} U_{k-1}(s), \tag{10}$$

where the coefficients $b_i^{(k)}$ and $c_i^{(k)}$ are of the forms

$$b_i^{(k)} = \frac{2}{\pi} \int_{-1}^{1} (1 - t^2)^{1/2} h_i(t) U_{k-1}(t)\, dt,$$

$$c_i^{(k)} = \frac{2}{\pi} \int_{-1}^{1} (1 - t^2)^{1/2} v_i(t) U_{k-1}(t)\, dt = \frac{1}{\pi} \int_{-1}^{1} p_i(t) U_{k-1}(t)\, dt.$$

Inserting (10) in (8) and using Proposition 3, we arrive at

$$a(s) \sum_{k=1}^{\infty} \left(\sum_{j=1}^{n} \lambda_{ij}^{(k)} b_j^{(k)} - c_i^{(k)} \right) U_{k-1}(s) = 0, \qquad s \in [-1, 1], \quad i = 1, \dots, n, \tag{11}$$

where

$$\lambda_{ij}^{(k)} = \frac{\sin(k(\omega_i - \omega_j))}{k \sin(\omega_i - \omega_j)}.$$

From the compatibility of systems (8) and (11), it follows that the system

$$\sum_{j=1}^{n} \lambda_{ij}^{(k)} b_j^{(k)} = c_i^{(k)} \qquad i = 1, \dots, n, \tag{12}$$

is also consistent.

The matrix $\Lambda_k = \left[\lambda_{ij}^{(k)}\right]$ can be singular (for example, for $k = 1$). In this case, the minimum normal solution of (12) can be calculated by using the matrix that is generalized inverse to Λ_k. Let us represent the solution of (11) as

$$h_i(s) = \sum_{k=1}^{\infty} U_{k-1}(s) \sum_{j=1}^{n} \eta_{ij}^{(k)} c_j^{(k)},$$

where $\eta_{ij}^{(k)}$ are the entries of Λ_k^{-1} or Λ_k^{+}. In result, we obtain (9).

The proof of Theorem 1 is complete. □

Corollary 1. *The norm of H has the form*

$$\|H\|^2 = \frac{1}{\pi} \sum_{k=1}^{\infty} \sum_{i,j=1}^{n} \eta_{ij}^{(k)} \int_{-1}^{1} U_{k-1}(s) p_i(s)\, ds \int_{-1}^{1} U_{k-1}(t) p_j(t)\, dt.$$

Proof. The proof follows from Theorem 1 and the equality

$$\|H\|^2 = \sum_{i=1}^{n} \int_{-1}^{1} h_i(s) p_i(s)\, ds.$$

The proof is over. □

If the angles ω_i of the projection directions are uniformly distributed $\omega_i = (i-1)\pi/n$, $i = \overline{1,n}$), then the analytical inversion of the matrix Λ_k is possible [28].

Proposition 4. *For $k < n$, the matrix Λ_k is singular and its generalized inverse Λ_k^{+} has the form*

$$\Lambda_k^{+} = k^2/n^2\, \Lambda_k.$$

In the case of arbitrary directions we use the numerical procedure **pinv** for pseudo-inversion of matrices from the standard program libraries of the MATLAB package. In recent works [6–8] containing also the literature surveys, the study that was started in classical works [5, 29, 30, 31] is continued; and the problems of smoothness, uniqueness, and stability of the sums of ridge functions and the SVD expansion of the Radon transform are important today as well.

3. INFORMATIVE DIRECTIONS OF PROJECTIONS

Let us assume that the image f is known as is the case for solving a direct problem or for the problems of image analysis and recognition. Then the data in the form of n projections $R_\omega f = (p_{\omega_1}, \ldots, p_{\omega_n})$ can be interpreted as the representatives or features of f. By varying the n-vector ω of directions, we can find the best approximation of f in the form

$$H_\omega = \sum_{j=1}^{n} h_{\omega_j}.$$

We can call one group of projections more informative than the other if the reconstruction based on the first data group is better than for the second one (in the sense of the chosen norm). The informative value of the projection data $R_\omega f$ can be estimated using the norm of the minimum solution H_ω by virtue of $\|f - H_\omega\|^2 = \|f\|^2 - \|H_\omega\|^2$.

Definition 3. We introduce the notation $Q(f,\omega) \equiv \|H_\omega(x,y)\|^2$ and call this quantity the *informative value of the projection set $R_\omega f$.*

If for two sets of projections $R_\omega f$ and $R_\alpha f$ registered for the sets of directions ω and α we have $Q(f,\omega) > Q(f,\alpha)$; then we say that the projections $R_\omega f$ are *more informative* than $R_\alpha f$. Recall that the informative value can be calculated based on projections and ridge functions as follows:

$$Q(f,\omega) = \|H_\omega\|^2 = \sum_{j=1}^{n} \int_{-1}^{1} p_{\omega_j}(s) h_{\omega_j}(s)\, ds. \tag{13}$$

For known f and given number of projections n, the most informative set of directions ω^0 can be found by the global search

$$\omega^0 = \arg\max_{\omega} Q(f,\omega). \tag{14}$$

It can be shown that the informative value of a single projection p_{ω_j} is calculated in the form

$$Q^0(f,\omega_j) \equiv 1/2 \int_{-1}^{1} (1-s^2)^{-1/2} p^2_{\omega_j}(s)\, ds. \tag{15}$$

In practice each projection p_{ω_j} is a discrete set of integrals along the rays. The problem arises of calculating the integrals $\int p_{\omega_j}(t) U_{k-1}(t)\, dt$ using the discrete data. Suppose that there are given m values $p_{jl} = p_{\omega_j}(t_l)$ of the projection p_{ω_j} at some points $t_l \in (-1,1)$, $l = 1,\dots,m$. In the case when

$$t_l = \cos\left(\frac{2l-1}{2m}\pi\right),$$

we can apply the Gauss–Chebyshev quadrature formula

$$\int_{-1}^{1} \frac{u(t)}{\sqrt{1-t^2}}\, dt \cong \frac{\pi}{m} \sum_{l=1}^{m} u(t_l).$$

Then

$$\int_{-1}^{1} p_{\omega_j}(t) U_{k-1}(t)\, dt \cong \frac{\pi}{m} \sum_{l=1}^{m} p_{\omega_j}(t_l) \sin\left(k\frac{2l-1}{2m}\pi\right)$$

and (9) is transformed to the form

$$h_{\omega_i}(s) = \frac{1}{m} \sum_{k=1}^{\infty} \sum_{j=1}^{n} \eta_{ij}^{(k)} U_{k-1}(s) \sum_{l=1}^{m} p_{jl} \sin\left(k\frac{2l-1}{2m}\pi\right).$$

In numerical inversion, the series (9) must be limited to a finite number of terms, and their number in the partial sum becomes the regularization parameter of this SVD decomposition. In our experiments, the truncation parameter for the infinite series is chosen to be equal to the number of samples (detectors) in the projection.

4. COMPUTATIONAL SCHEME OF THE TEXTURE DECOMPOSITION

The working hypothesis is that regular textures are fairly well approximated by the sum of rather small ($M = 2,3,\dots,10$) number of informative ridge functions. The number M is selected for each texture under study by modeling. The typical dimensions of the $n \times n$ matrix of the texture image are $n = 256,\dots,512$ and larger. Practice shows that for such n the calculation of the Radon transform R_ω as the matrix of dimension $n \times n$ has sufficient resolution with respect to angle.

Calculate the complete sinogram R_ω and find M informative projections in the directions $\alpha = (\alpha_1,\dots,\alpha_M)$, so that α is a subset of the set of angles ω. The set α can be obtained by a complete combinatorial search of M angles among the set of n directions ω and calculation of the informative

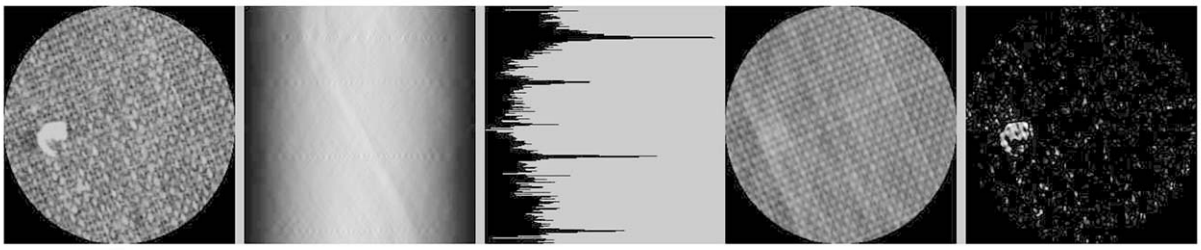

Fig. 1. Textile, sample E2R10.jpg from the database GLSR [32]: (a) the test object f, $n = 256$ and $\|f\|^2 = 65903$; (b) the sinogram of size $n \times n$; (c) the graph of informative values Q^0; (d) the reconstruction of H_α by four projections selected in the directions $\alpha = (24°, 58°, 113°, 170°)$, $\|H_\alpha\|^2 = 63733$ and $\|H_\alpha\|^2/\|f\|^2 = 0.97$; and (e) the absolute value of difference $|f - H_\alpha|$ of images in plots (a) and (d).

value Q using (13) and (14) or by a fast search for local maxima of informative values Q^0 of individual projections by (15). Then we calculate the minimum solution H_α.

If there is a defect on the texture, it will show itself in the reconstruction H_α as some more smooth region due to the integral nature of the Radon transform and the regularization of the procedure of the truncated singular value decomposition. Having the original image of the texture with irregularity and an informative approximation with a suppressed defect, we can, by exploring their difference, identify the defect because the non-defective regions are cancelled out. The regions with a significant difference are determined as indicators of anomaly and are generally detected by statistical methods.

5. NUMERICAL EXPERIMENTS WITH TEXTURES

In computational experiments, we used some texture samples from the two open databases [32, 33] of textile images. The selected texture was bounded by a circular window in a square-shaped image of size $n \times n$. Given the image f, we numerically generated n projections that were uniformly distributed in the range $[0, \pi)$; i.e., with the discreteness of $180/n$ degrees. Each projection had n readings, so the Radon transform, or sinogram, was of size $n \times n$. The informative values Q^0 of n individual projections were calculated by (15); and then, by studying the local maxima, we could select M projections of α by which the SVD reconstruction H_α was calculated. The selection of projections for subsequent use in the reconstruction was carried out automatically by the search for local maxima according to the number of pre-defined informative projections.

The results of the experiment for each sample of the selected test image are illustrated in Figs. 1 and 2 in the form of five consecutive images from left to right as follows:

(a) test image f;

(b) the Radon transform (sinogram) where the projections are arranged line by line sequentially from top to bottom and the samples (detectors) make up the horizontal axis;

(c) the informative value of individual projection, the graph of Q^0 is depicted vertically from top to bottom for easy comparison with the sinogram;

(d) the reconstruction or minimum normal solution H_α;

(e) difference between the test image and the normal solution $|f - H_\alpha|$.

The numerical experiments conducted have shown that the search for the set of angles ω^0 of (14), at which the global maximum of joint informative value Q of (13) is reached, can be accelerated by using one-dimensional search for M local maxima of informative value Q^0 of individual projections (15). Our experiments on some textures from databases [32, 33] and other textile images demonstrated that, in the case of regular textures under study, using the quick informativeness criterion Q^0 for individual projections yields the results comparable to those of the global search.

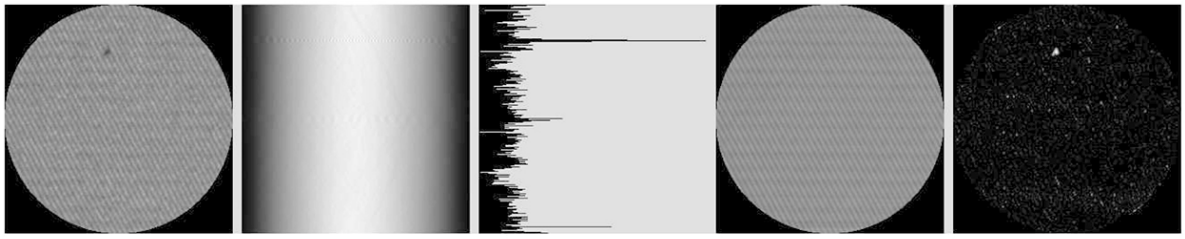

Fig. 2. Textile, sample 0057_019_06.png from the database AITEX [33]: (a) the test object f, $n = 256$ and $\|f\|^2 = 60495$; (b) the sinogram of size $n \times n$; (c) the graph of n informative values Q^0; (d) the reconstruction of H_α by the three projections in the directions $\alpha = (28^\circ, 89^\circ, 128^\circ)$, $\|H_\alpha\|^2 = 60202$ and $\|H_\alpha\|^2/\|f\|^2 = 0.99$; and (e) the absolute value of difference $|f - H_\alpha|$ of images in plots (a) and (d).

CONCLUSION

The article explores the possibilities of using the singular value decomposition of the Radon transform in modeling the regular textures in images. Anisotropy in certain directions is considered as a characteristic feature of these structures. As a quantitative estimation of the quality of the image approximation by the sum of rather small number of ridge functions, the criterion of the informative value of the projection data is used. The computational experiments are conducted on some images of real textures from the databases used in the textile industry for testing the methods and algorithms of detecting defects.

The algorithm of the singular value decomposition of the Radon transform demonstrated the efficiency and fairly accurate reconstruction of smooth approximations of regular textures. Unlike most heuristic image processing approaches, the proposed method has an analytical justification. The limits of application of the approach, as well as the ways to subdivide the textures into regular and irregular ones, remain topical problems and are the subject of further research. The method can be used in technical vision systems, and we plan to improve this approach in the future in the direction of improving noise robustness.

FUNDING

The authors were supported by the State Task to the Institute of Computational Mathematics and Mathematical Geophysics of the Siberian Branch of the Russian Academy of Sciences (project no. 0251–2021–0003) and by the Ministry of Education and Science of the Republic Kazakhstan (project no. AP05133873).

REFERENCES

1. F. Natterer, *The Mathematics of Computerized Tomography* (Wiley, New York, 1985; Mir, Moscow, 1990).
2. P. Bachiller-Burgos, L. J. Manso, and P. Bustos, "A Variant of the Hough Transform for the Combined Detection of Corners, Segments, and Polylines," J. Image Video Proc. **2017**, 32 (2017).
3. V. G. Bondur and A. T. Zverev, "A Method Earthquake Forecast Based on the Lineament Analysis of Satellite Images," Dokl. Akad. Nauk **402** (1), 98–105 (2005) [Dokl. Earth Sci. **402** (4), 561–567 (2005)].
4. A. S. Alekseev, I. G. Kazantsev, and V. P. Pyatkin, "A Tomographic Approach to Highlighting Lineaments in Aerospace Imagery," Issled. Zemli iz Kosmosa No. 5, 99–103 (1988).
5. B. F. Logan and L. A. Shepp, "Optimal Reconstruction of a Function from Its Projections," Duke Math. J. **42**, 645–659 (1975).
6. A. Pinkus, *Ridge Functions* (Univ. Press, Cambridge, 2015).
7. V. E. Ismailov, "Approximation by Sums of Ridge Functions with Fixed Directions," Algebra i Analiz **28** (6), 20–69 (2016).
8. S. V. Konyagin, A. A. Kuleshov, and V. K. Mayorov, "Some Problems in the Theory of Ridge Functions," Trudy Mat. Inst. Steklov. **301**, 155–181 (2018) [Proc. Steklov Inst. Math. **301** (1), 144–169 (2018)].
9. R. M. Haralick, "Statistical and Structural Approaches to Texture," Proc. IEEE **67** (5), 786–804 (1979).

10. P. P. Koltsov, "Comparative Study of Algorithms for the Selection and Classification of Textures," Zh. Vychisl. Mat. Mat. Fiz. **51** (8), 1561–1568 (2011) [J. Comput. Math. Math. Phys. **51** (8), 1561–1568 (2011)].
11. F. Tomita and S. Tsuji, *Computer Analysis of Visual Textures* (Kluwer Acad. Publ., Boston, 1990).
12. S. V. Ershov, V. Reimer, E. N. Kalinin, and T. Gries, "Development of a Computer Vision System for Measuring the Fiber Orientation in Braided Structures," Izv. Vyssh. Uchebn. Zaved. Tekhnol. Tekstil. Prom. No. 5, 204–208 (2019).
13. W. H. Nyan, *Quality Control Information System for the Production of Multilayer Woven Fabrics Based on the Processing of Their Images*, Avtoreferat of Candidates Dissertation on Techn. Nauk (Moscow, 2020).
14. *Applications of Computer Vision in Fashion and Textiles* (Woodhead Publ., Cambridge, 2018).
15. S. Thomassey and X. Zeng, *Artificial Intelligence for Fashion Industry in the Big Data Era* (Springer, Singapore, 2018).
16. P. M. Mahajan, S. R. Kolhe, and P. M. Patil, "A Review of Automatic Fabric Defect Detection Techniques," Adv. Comput. Research **1** (2), 18–29 (2009).
17. H. Y. T. Ngan, G. K. H. Pang, and N. H. C. Yung, "Automated Fabric Defect Detection: A Review," Image Vis. Comput. **29** (7), 442–458 (2011).
18. K. Hanbay, M. F. Talu, and Ö. F. Özgüven, "Fabric Defect Detection Systems and Methods. A Systematic Literature Review," Optik **127** (24), 11960–11973 (2016).
19. B. K. Behera, "Image-Processing in Textiles," Textile Progress **35** (2–4), 1–193 (2004).
20. J. Zhang, B. Xin, and X. Wu, "A Review of Fabric Identification Based on Image Analysis Technology," Textiles and Light Industrial Science and Technology (TLIST) **2** (3), 120–130 (2013).
21. C.-H. Chan and G. K. H. Pang, "Fabric Defect Detection by Fourier Analysis," IEEE Trans. Ind. Appl. **36** (5), 1267–1276 (2000).
22. L. A. Vese and S. J. Osher, "Modeling Textures with Total Variation Minimization and Oscillating Patterns in Image Processing," J. Sci. Computing **19**, 553–572 (2003).
23. C. Chaudhari, R. K. Gupta, and S. Fegade, "A Hybrid Method of Textile Defect Detection Using GLCM, LBP, SVD, and Wavelet Transform," Internat. J. Recent Technol. Eng. **8** (6), 5356–5360 (2020).
24. L. Peng, J. Liang, X. Shen, M. Zhao, and L. Sui, "Textile Fabric Defect Detection Based on Low-Rank Representation," Multimedia Tools and Applications **78** (1), 99–124 (2019).
25. M. K. Ng, H. Y. T. Ngan, X. Yuan, and W. Zhang, "Lattice-Based Patterned Fabric Inspection by Using Total Variation and Sparsity with Low-Rank Representations," SIAM J. Imaging Sci. **10** (4), 2140–2164 (2017).
26. Z. Liu, B. Wang, C. Li, M. Yu, and S. Ding, "Fabric Defect Detection Based on Deep-Feature and Low-Rank Decomposition," J. Eng. Fibers and Fabrics **15**, 1–12 (2020).
27. J. Cao, J. Zhang, Z. Wen, N. Wang, and X. Liu, "Fabric Defect Inspection Using Prior Knowledge Guided Least Squares Regression," Multimedia Tools and Applications **76** (3), 4141–4157 (2017).
28. I. G. Kazantsev, "Tomographic Reconstruction from Arbitrary Directions Using Ridge Functions," Inverse Problems **14**, 635–645 (1998).
29. M. E. Davison, "A Singular Value Decomposition for the Radon Transform in n-Dimensional Euclidian Space," Numer. Funct. Anal. Optim. **3**, 321–340 (1981).
30. M. E. Davison and F. A. Grunbaum, "Tomographic Reconstruction with Arbitrary Directions," Communs. Pure Appl. Math. **34**, 77–120 (1981).
31. A. K. Louis, "Optimal Sampling in Nuclear Magnetic Resonance (NMR) Tomography," J. Comput. Assist. Tomogr. **6** (2), 334–340 (1982).
32. *Fabric Defect Inspection GLSR Dataset*, URL: https://github.com/jjcao/Fabric-Defect-Inspection-GLSR.
33. J. Silvestre-Blanes, T. Albero-Albero, I. Miralles, R. Pérez-Llorens, and J. Moreno, "A Public Fabric Image Database for Defect Detection," AUTEX Research J. **19** (4), 363–374 (2019). URL: https://www.aitex.es/afid/